Journal of Radiation Research, Vol. 64, No. 1, 2023, pp. 11–23
https://doi.org/10.1093/jrr/rrac060
Advance Access Publication: 10 October 2022

Epigenetic regulation of RARB overcomes the radio-resistance of colorectal carcinoma cells via cancer stem cells

Yuxian Shu[1], Jun Lan[2], Zhaobing Hu[3], Weiguo Liu[4] and Rongfeng Song[4,*]

[1]Department of Comprehensive Radiotherapy, Jiangxi Cancer Hospital, Nanchang 330029, Jiangxi, P.R. China
[2]Department 1 of General Surgery, Jiangxi Gao'an People's Hospital, Gao'an 330800, Jiangxi, P.R. China
[3]Department of Oncology, Jingdezhen Second People's Hospital, Jingdezhen 333000, Jiangxi, P.R. China
[4]Department of Gastroenterology, Jiangxi Cancer Hospital, Nanchang 330029, Jiangxi, P.R. China
*Corresponding author. Department of Gastroenterology, Jiangxi Cancer Hospital, No. 519, Beijing East Road, Qingshanhu District, Nanchang 330029, Jiangxi, P.R. China. Email: songrf11251@163.com; Tel/Fax: 13879172671
(Received 28 April 2022; revised 19 July 2022; editorial decision 24 August 2022)

ABSTRACT

Cancer stem cells (CSCs) are able to survive after cancer therapies, leading to cancer progression and recurrence in colorectal carcinoma (CRC). Therapies targeting CSCs are believed to be promising strategies for efficiently eradicating cancers. This study was to investigate that how retinoic acid receptor beta (RARB) affected the biological characteristics of CSCs and radio-resistance in CRC and the epigenetic mechanism. The sensitivity of CSCs isolated from HCT116 cells to radiotherapy was reduced compared with the parental cells. Using database querying, we found that RARB was one of the most significantly downregulated gene in radio-resistant cells in CRC. Also, RARB was poorly expressed in our isolated CSCs, and overexpression of RARB inhibited the properties of CSCs and enhanced radiotherapy sensitivity. Mechanistically, the methylation of RARB was higher in CSCs compared with HCT116 cells, which was significantly reduced after the application of DNA methylation inhibitor 5-azacytidine (5-azaC). DNA methyltransferases (DNMT1) was found to be recruited into the RARB promoter. 5-AzaC treatment inhibited DNMT1 activity and improved radiotherapy sensitivity by promoting RARB expression. Our results imply that inhibition of DNMT1 can display a new mechanism for the epigenetic mediation of RARB in radio-resistant CRC.

Keywords: colorectal carcinoma (CRC); cancer stem cells (CSC); retinoic acid receptor beta (RARB); DNA methyltransferases (DNMT1); radiotherapy sensitivity

INTRODUCTION

Colorectal carcinoma (CRC) represents the second most common cause of cancer-associated death in the US in 2020 [1]. According to the latest statistics, long-term declines in mortality have slowed for CRC, causing an estimated 52 980 deaths in the US in 2021 [2]. Surgery, chemotherapy and radiotherapy have appreciably prolonged the survival of patients with CRC [3]. However, the development of cancer cells resistance to radiotherapy is one of the major issues for the clinical management of CRC patients, leading to tumor recurrence and an unfavorable prognosis [4]. Therefore, it is urgent to study the molecular mechanisms underlying radiotherapy in CRC.

It is well-known that cancer stem cells (CSCs) are resistant to treatment and can cause tumor relapses [5]. CSCs are a subpopulation of cells within tumors that possess the characteristics of self-renewal, quiescence, differentiation and the capacity to recapitulate the parental tumor when transplanted into a host [6]. In this study, we identified retinoic acid receptor beta (RARB) as a significantly downregulated gene in CRC cells resistant to radiation relative to wild type CRC cells in the GEO database. Consistently, the promoter methylation of RARB was enhanced in CRC cells compared to normal FHC cells [7]. Therefore, we wondered whether the potential effects of RARB on mediating radio-resistance was associated to the stemness of CSC. Epigenetic programs led to gene expression regulation and have been suggested as main drivers to self-renewal and differentiation of CSCs [8]. More importantly, DNA methylation, histone modification and non-coding RNAs identified in the control of

signaling pathways in CSCs have provided greater promise in the improvement of understanding cancer radio-resistance [9]. Intriguingly, RARB was found to be one of seven genes with hypermethylated promoter regions in CRC [10]. Based on these previous findings, we focused on the correlation between DNA methylation of RARB and radio-resistance in the present study. DNA methylation at the 5-position of cytosine, catalyzed by DNA methyltransferases (DNMTs), is a major epigenetic modification in mammals, and DNMT1 is a main enzyme responsible for maintenance of the DNA methylation pattern [11]. For instance, the transcriptional repression of *PEPT1* in CRC was found to be related to DNMT1-mediated DNA methylation of the proximal promoter region [12]. The regulatory mechanism between DNMT1 and RARB, however, is unclear. As a consequence, the purpose of this study was to probe whether DNMT1 affected the biological characteristics of CSCs in CRC via maintenance of methylation of RARB.

MATERIALS AND METHODS

Cell culture and sorting of CSCs

Human CRC cells HCT116 (CCL-247™) and normal human intestinal epithelial cells (HIEC-6, CRL-3266™) were from American type culture collection (Manassas, VA, USA) and cultured in DMEM (11 965 092, Gibco, Carlsbad, CA, USA) containing 10% FBS (16 140 071, Gibco) in an incubator at 37°C with 5% CO_2. When the confluence reached 90%, the cells were trypsinized and passaged. Cells at the logarithmic growth phase were used for following assays.

Cells with CSC characteristics were isolated from HCT116 cells and identified by flow cytometry. In short, HCT116 cells were harvested and incubated with antibodies to CD133 (1:100, ab252129, Abcam, Cambridge, UK) and CD44 (1:40, ab27285, Abcam) for nearly 1 h. Subsequently, the resuspended in 100 μL fluorescence-activated cell sorter buffer, and the percentage of positive cells was assessed using a BD FACSCalibur flow cytometry system (BD Biosciences, San Diego, CA, USA).

Cell transfection and treatment

The cells were transfected using Lipofectamine 2000 (11 668 030, Invitrogen Inc., Carlsbad, CA, USA) as per the manufacturer's instructions. The siRNA targeting DNMT1 mRNA (si-*DNMT1*), DNMT3A mRNA (si-*DNMT3A*), DNMT3B mRNA (si-*DNMT3B*), RARB mRNA (si-RARB) and negative control (si-NC) were acquired from Shanghai GenePharma Co., Ltd. (Shanghai, China). The sequences of the siRNAs are shown in Table 1. The full-length RARB cDNA was subcloned into pcDNA3.1 vector (Invitrogen) for the construction of RARB overexpression (oe-RARB), with the empty vector as a negative control (oe-NC). After seeding and plating in 6-well plates for 1 d, the cells were transfected with the plasmids. After 48 h of transfection, the cells were stored for later use. Transfection efficiency was determined by RT-qPCR.

To suppress the expression of DNMT1, the cells were treated with 10 μM 5-aza-2′-deoxycitidine (5-AzaC) (189 825, Sigma-Aldrich Chemical Company, St Louis, MO, USA) 3 days before transfection. An equal volume of dimethylsulfoxide (DMSO) was applied as a control.

Table 1. SiRNAs sequence

siRNAs	Sequence
si-DNMT1#1	5'-CAAAGATTTGGAAAGAGACAGCTTA-3′
si-DNMT1#2	5'-CAGCACAAACTGACCTGCTTCAGTG-3′
si-DNMT3A#1	5'-CAGTGGTGTGTGTTGAGAAGCTGAT-3′
si-DNMT3A#2	5'-CCACGTACAACAAGCAGCCCATGTA-3′
si-DNMT3B#1	5'-CAGTGGTTTGGCGATGGCAAGTTCT-3′
si-DNMT3B#2	5'-GAGACTCATTGGAGGACCAGCTGAA-3′
si-RARB#1	5'-GACAAATCATCAGGGTACCACTATG-3'
si-RARB#2	5'-CACCGAGATAAGAACTGTGTTATTA-3'

Note: siRNA, small interfering RNA; DNMT, DNA methyltransferase; RARB, retinoic acid receptor beta.

Cell counting kit-8 (CCK-8)

Cells (3×10^3 cells/well) were grown in 96-well plates for 12 h and irradiated with 6 MV X-rays at 37°C at 0, 2, 4, 6 and 8 Gy. After 24 h of irradiation (IR), 10 μL CCK-8 reagent (C0037, Beyotime Institute of Biotechnology, Shanghai, China) was supplemented to each well and incubated for 2 h at 37°C and 5% CO_2. The optical density (OD) value was measured at 450 nm using a microplate reader. The dose of 6 Gy was used in all subsequent experiments.

RT-qPCR

For RNA extraction, fresh tissues and cells were lysed using TRIzol reagent (15 596 026, Invitrogen) and purified using the RNeasy Mini Kit (Qiagen, Valencia, CA, USA). Total RNA from cells or tissues was extracted and used for reverse transcription according to the instructions of the PrimeScript™ RT Kit (#RR037A, TaKaRa, Beijing, China). Real-time polymerase chain reaction (PCR) was performed using TB Green® Premix Ex Taq™ II (#RR820A, TaKaRa) and a real-time fluorescence quantitative PCR instrument (ABI 7500, ABI, Foster City, CA, USA). Gene expression was normalized to β-actin to calculate relative expression using the $2^{-\Delta\Delta Ct}$ method. The primer sequences used in this study were listed as below: RARB, forward: 5'-CAAACCGAATGGCAGCATCG-3′; reverse: 5'-TCTGCGGAAAAAGCCCTTACA-3′; *β-actin*, forward: 5'-AACTGGGACGACATGGAGAAAA-3′; reverse: 5'-GGATAGCA CAGCCTGGATAGCA-3′.

Western blot

Total proteins were isolated from cells or tissues using radioimmunoprecipitation cell lysis buffer (BB-3201-1, BestBio Ltd., Shanghai, China), separated by SDS-PAGE, and electrotransferred onto polyvinylidene fluoride membrane. The membranes were sealed with a sealing solution for 60 min and incubated overnight at 4°C with the primary rabbit antibodies to RARB (1:1000, ab53161, Abcam), β-actin (1:5000, ab8227, Abcam), CD133 (1:1000, ab216323, Abcam), CD44 (1:1000, ab243894, Abcam), Nanog (1:2000, ab109250, Abcam), DNMT1 (1:1000, ab19905, Abcam), DNMT3A (1:1000, ab188470, Abcam) and DNMT3B (1:500, ab2851, Abcam). The next day, the membranes were incubated with horseradish peroxidase-conjugated goat anti-rabbit IgG (1:5000, ab6721, Abcam) for 60 min at 37°C and developed with enhanced chemiluminescence reagent.

Spheroid formation assay

After IR at a dose of 6 Gy, a total of 1×10^4 CSCs were seeded in 96-well low-adsorption plates and incubated with serum-free DMEM-F12. The medium was then supplemented with 20 ng/mL epidermal growth factor and 20 ng/mL fibroblast growth factor-β and subjected to semi-quantitative medium renewal at an interval of 2 days. After 10–14 days, spheroids $\geq$50 μm in diameter were counted microscopically.

Clonogenic cell survival assay

Cells without radiation and after 6 Gy dose of radiation were resuspended with 1 mL of culture medium. The cell suspension (1 mL) was mixed with 1 mL of 0.7% agarose in DMEM at 1×10^4 cells/100 cm^2. The cell suspension was seeded into 100-mm containers pre-covered with 0.7% agarose. The medium (2–3 mL) was supplemented dropwise to the surface of the agarose for incubation, and the medium was changed at an interval of 2 to 3 days. Cells were counted after 1 month, and opaque spots with $\geq$ 50 cells were deemed as a colony. Images were acquired with a DMM-300D microscope (Caikon, Shanghai, China). Survival fraction = number of colonies formed from cells after radiation/number of colonies formed from cells not irradiated $\times$ 100%.

Flow cytometry

After IR at a dose of 6 Gy, the cells were plated in 6-well plates at 4×10^5 cells/well. After 48 h, the cells were harvested. The cell apoptosis was measured with the Annexin V-FITC Apoptosis Staining/Detection Kit (ab14085, Abcam) according to the manufacturer's instructions, followed by flow cytometric analysis (CYTOMINCS FC500, Becton, Dickinson and Company, Franklin Lakes, NJ, USA).

Bisulfite sequencing PCR and methylation-specific PCR

For methylation-specific PCR (MSP) analysis, genomic DNA was isolated from cells using the Genomic DNA Purification Kit (K0512, Thermo Scientific™, Rockford, IL, USA) and modified with the EpiTect Fast DNA Bisulfite Kit (59 802, Qiagen, Hilden, Germany). Primer sequences of RARB promoter were as follows: Methylated, 5'-GAATTTAATAGATAGAAAGGCGTAT-3′ (forward) and 5'-GAAACGCTACTCCTAACTCACG-3′ (reverse); Unmethylated, 5′-AAGGAATTTAATAGATAGAAAGGTGTAT-3′ (forward), and 5'-AACCAAAACACTACTCCTAACTCACAT-3′ (reverse). The PCR product was 177 bp and then visualized in a 2% agarose gel. In the MSP results, the presence of the M band represents methylation, while the presence of the U band represents unmethylation.

For bisulfite sequencing PCR (BSP) analysis, the promoter region of RARB was analyzed. The primer sequences were as follows: 5′-TTTTTTGTTTATTTTAAAAGTATTTTTTGT-3′ (forward) and 5'-AAATTCTCACAAAACTTAAAAACTCC-3′ (reverse). The PyroMark Q96 ID System and software (Qiagen) were applied for sequencing reactions and methylation level quantification.

ChIP assay

Enrichment of DNMT1 in the RARB promoter region was assessed using the ChIP kit (17 409, Millipore Corp, Billerica, MA, USA). CSCs were incubated until a cell confluence reached 70–80% and then mixed in 1% formaldehyde for 10 min to cross-link deoxyribonucleic acid and proteins. The cells were sonicated to generate 200 to 1000 bp DNA fragments. After centrifugation at 4°C, the supernatant was incubated with antibodies specific to DNMT1 (1 μg/mL, ab19905, Abcam) or negative control IgG (1 μg/mL, ab172730, Abcam). The DNA was de-crosslinked overnight at 65°C, extracted, purified and collected for PCR analysis.

Xenograft tumor in nude mice

Animal experiments were permitted by the Ethical Committee of Jiangxi Cancer Hospital and performed as per the guidelines for the care and use of laboratory animals. To establish a xenograft tumor model, lentivirus overexpressing RARB (LV-oe-RARB), lentivirus encoding shRNA-RARB (LV-sh-RARB) and the corresponding controls (LV-oe-NC, LV-sh-NC) were purchased from Shanghai Genechem Co., Ltd. (Shanghai, China). CSCs were infected with lentivirus at 5 mg/mL of polybrene for 48 h. Finally, stable CSCs were screened by treatment with puromycin (5 μg/mL) for 2 weeks. For *in vivo* tumorigenesis experiments, 36 male BALB/c nude mice (4–6 weeks old, 18–25 g) were purchased from Hunan SJA Laboratory Animal Co., Ltd. (Changsha, Hunan, China). The nude mice were randomly categorized into six groups ($n = 6$), and 150 μL PBS containing 1×10^7 stable CSCs was injected subcutaneously in the left inguinal region. To assess the impact of 5-AzaC on tumor growth, the nude mice were treated intraperitoneally with 5-AzaC at 0.5 mg/kg or DMSO every other day for 4 weeks when tumors reached 3 mm in diameter.

When the tumor diameter reached approximately 8.0 mm (range from 7.7 to 8.2 mm), the nude mice were subjected to IR using a small animal irradiator (Co-V, Theratron 780; MDS Nordion, Ottawa, Canada) with a cobalt-60 source. Subsequently, nude mice immobilized in the fixture were exposed to 5 Gy IR at 0.955 Gy/min. The day of radiotherapy was recorded as day 0, and tumor growth was measured every 4 days. The tumor volume (V) was determined as: $V = 1/2 \times$ larger diameter $\times$ (smaller diameter)^2. After 28 days, the mice were euthanized by intraperitoneal injection of an overdose of sodium pentobarbital (150 mg/kg), then the tumors were removed. Tumor weights were recorded, and subsequent experiments were performed.

TUNEL assay

The Colorimetric TUNEL Apoptosis assay kit (C1091, Beyotime Institute of Biotechnology) was used as per the manufacturer's instructions. Tumor sections were incubated with 3% H_2O_2 and TUNEL reaction mixture. The sections were rinsed and stained using diaminobenzidine. Hematoxylin was used for counter-staining. Under a light microscope (Olympus, Tokyo, Japan), the number of TUNEL-positive cells from six random fields of view was counted at a magnification of $\times$400. Apoptosis rate was calculated as the percentage of TUNEL-positive cells relative to total cells.

Statistical analyses

All the data were analyzed using SPSS 21.0 (IBM, Armonk, NY, USA) and GraphPad Prism 9.0 (GraphPad Software Inc., San Diego, CA, USA). The measurement data were exhibited as mean $\pm$ SD. Differences between two groups were compared by paired or unpaired *t*-test, while that among multiple groups was analyzed by one-way or

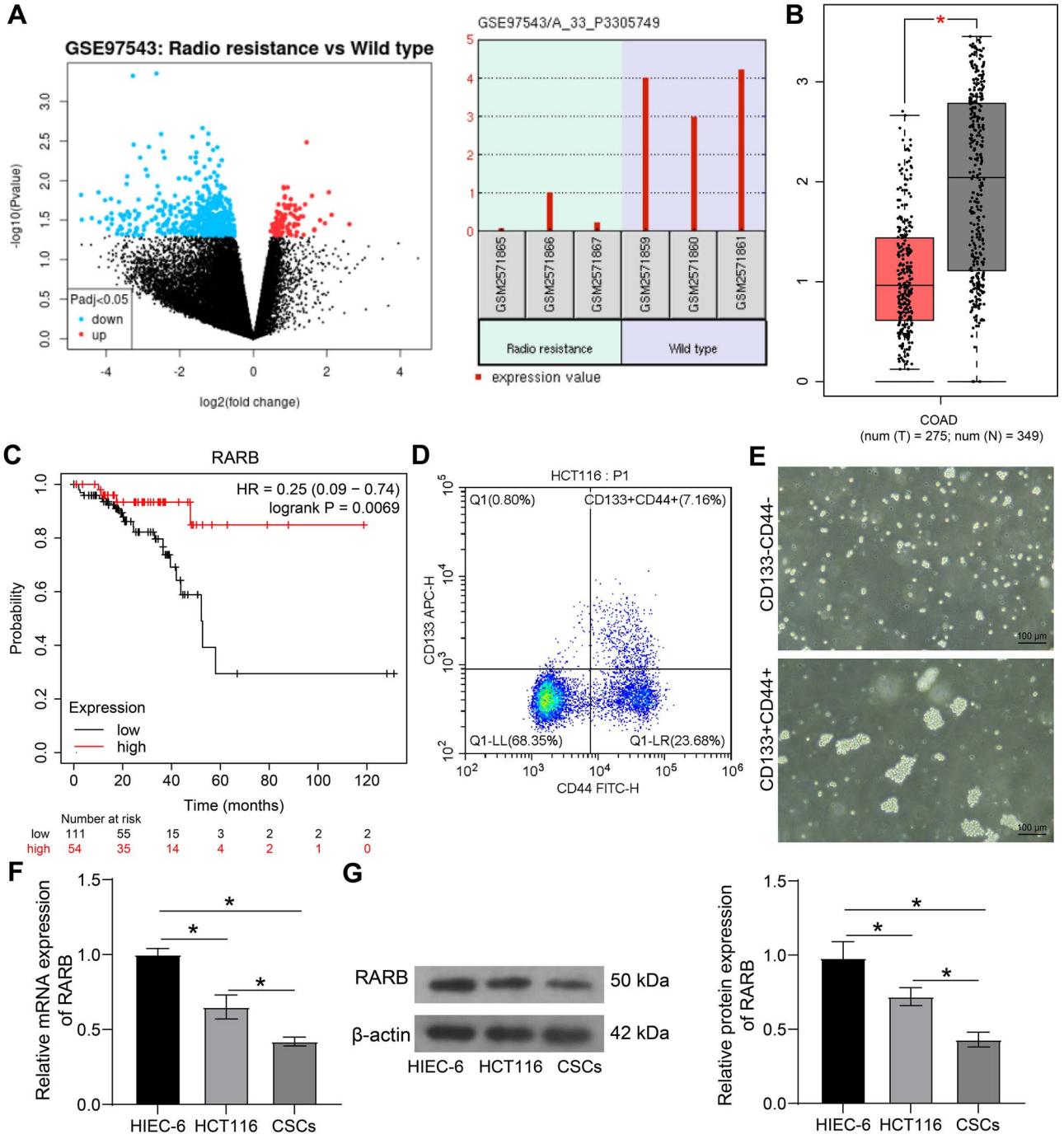

Fig. 1. RARB expression is downregulated in CRC. (A) Screening of differently expressed genes in the GSE97543 data set. (B) Downregulation of RARB in CRC found in GEPIA (http://gepia.cancer-pku.cn/index.html). (C) The survival analysis of CRC patients with different RARB expression using Kaplan–Meier Plotter (http://kmplot.com/analysis/index.php?P=background). (D) Isolation and identification of $CD133^{+}CD44^{+}$ cells with CSC characteristics from HCT116 cells using flow cytometry. (E) The spheroid formation of $CD133^{-}CD44^{-}$ and $CD133^{+}CD44^{+}$ cells. (F-G) Detection of RARB expression in HIEC-6 cells, HCT116 cells and CSCs using RT-qPCR (F) and Western blot (G). The statistical data were expressed as mean ± SD. The differences between two groups were compared by unpaired *t* test, and the others were compared by one-way ANOVA. *, $P < 0.05$.

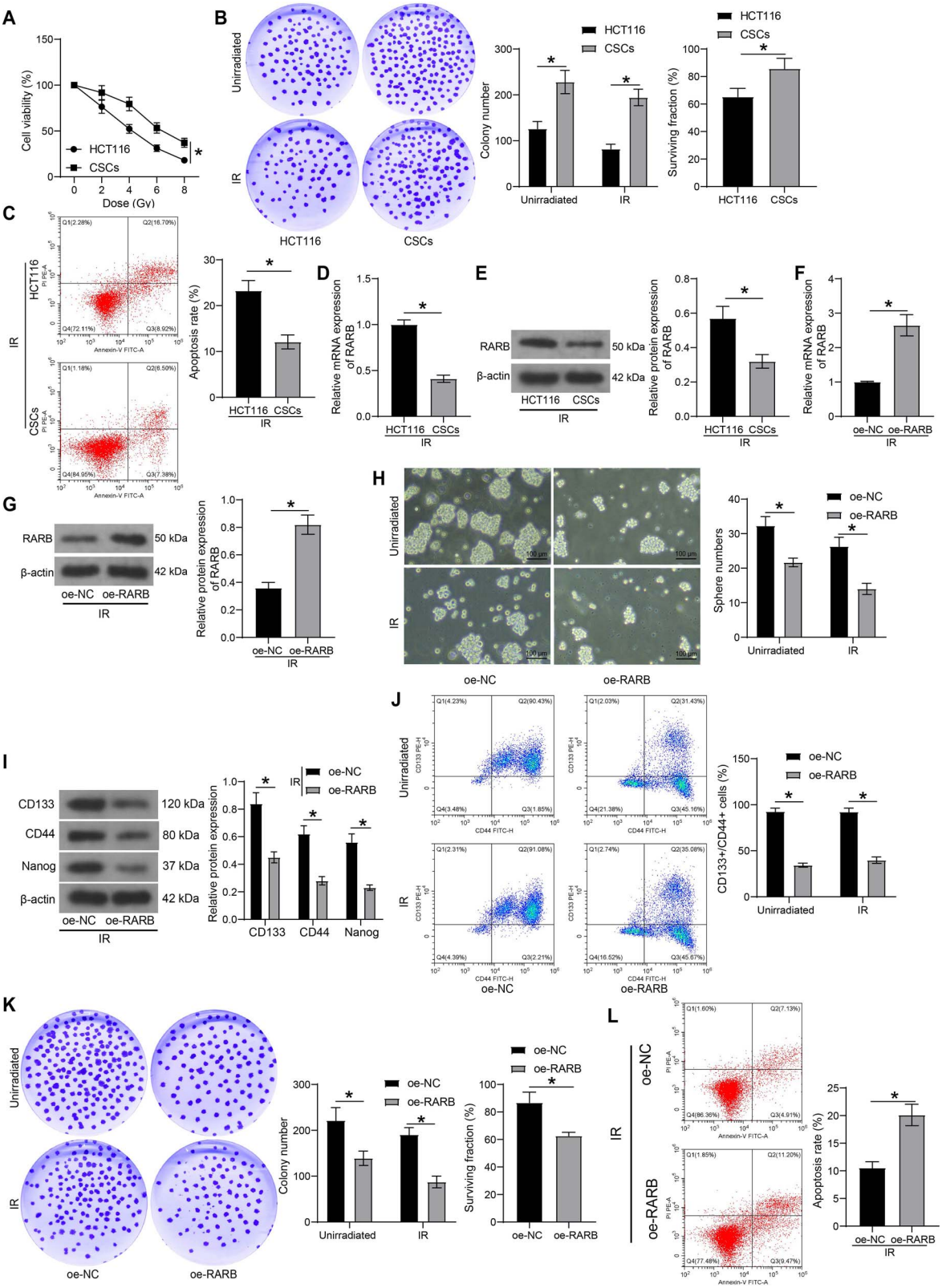

Fig. 2. Overexpression of RARB inhibits the stem cell properties of CSCs and improves radiotherapy sensitivity. (A) The cellular viability of HCT116 cells and CSCs at different IR doses (0, 2, 4, 6, 8 Gy) measured using CCK-8 assay. (B) The clonogenic ability and survival fraction of HCT116 cells and CSCs with or without radiotherapy (6 Gy) treatment. (C) The apoptosis rate of

two-way ANOVA, followed by Tukey's post hoc-tests. The threshold for statistical significance was set at $P < 0.05$.

RESULTS

RARB is poorly expressed in CSC isolated from CRC cells

Three CRC cell samples (GSM2571859 ~ GSM2571861) and three radiotherapy-resistant CRC cell samples (GSM2571865 ~ GSM2571867) were first selected from the GEO data set GSE97543 to screen for differentially expressed genes in radio-resistance. RARB (GPL13497 platform number: A_33_P3305749) was screened out to be significant poorly expressed in radiotherapy-resistant cells (Fig. 1A). RARB expression was much lower in CRC by GEPIA (http://gepia.cancer-pku.cn/index.html) (Fig. 1B). Moreover, the survival of patients with high RARB expression was much higher than that of patients with low RARB expression by Kaplan–Meier Plotter (http://kmplot.com/analysis/index.php?P=background) (Fig. 1C). It was suggested that RARB is significantly associated with CRC progression.

We identified $CD133^+CD44^+$ cells with CSC characteristics from HCT116 cells using flow cytometric analysis. As shown in Fig. 1D, $CD133^+CD44^+$ accounted for 7.16% in HCT116 cells. The sorted $CD133^+CD44^+$ cells and $CD133^-CD44^-$ cells were cultured separately in serum-free stem cell induction medium. $CD133^+CD44^+$ cells were found to grow in suspension with more spheroid formation and larger spheroids size compared with $CD133^-CD44^-$ cells (Fig. 1E), indicating that the sorted CSCs ($CD133^+CD44^+$ cells) showed high self-renewal capacity. Then, the expression of RARB in HIEC-6 cells, HCT116 cells and CSCs was detected by RT-qPCR and Western blot. The RARB expression was considerably reduced in CRC cells relative to the HIEC-6 cells, and the reduction was more pronounced in CSCs (Fig. 1F–G). It indicates that RARB is poorly expressed in CSCs.

RARB inhibits the stem cell properties of CSCs and improves radiotherapy sensitivity

To confirm whether CSCs correlated with sensitivity to radiotherapy, we performed radiotherapy on HCT116 cells and CSCs, respectively. The CCK-8 assay was performed to assess cell viability at different IR doses (0, 2, 4, 6 and 8 Gy). The cell viability of CSCs was significantly promoted versus the HCT116 cells (Fig. 2A), and 6 Gy was selected for subsequent experiments. Then, the clonogenic formation and apoptosis of the cells were assessed by clonogenic cell survival assay and flow cytometry, respectively. The clonogenic number and survival fraction of CSCs was significantly increased compared with HCT116 cells (Fig. 2B). In contrast, the apoptosis rate was significantly decreased (Fig. 2C), suggesting that CSCs have reduced sensitivity to radiotherapy compared with HCT116 cells. Meanwhile, RT-qPCR and Western blot were carried out to evaluate the RARB expression in the cells. The expression of RARB was significantly reduced in CSCs after IR treatment compared with HCT116 cells (Fig. 2D–E).

To confirm whether abnormally low RARB expression in CSCs correlated with sensitivity to radiotherapy, CSCs transfected with oe-NC or oe-RARB were treated with radiotherapy (6 Gy). The results of RT-qPCR and Western blot showed that the transfection of oe-RARB was successful (Fig. 2F–G). The results of spheroid formation assay evidenced that the spheroid-forming ability of CSCs was significantly reduced after transfection of oe-RARB compared to the oe-NC transfection (Fig. 2H), accompanied by downregulation of CSCs-associated factors CD133, CD44 and Nanog (Fig. 2I) and declines in the fraction of $CD133^+CD44^+$ cells (Fig. 2J). The results of clonogenic cell survival assay and flow cytometry showed that the cells in the oe-RARB group had significantly lower clonogenic ability and survival fraction (Fig. 2K) and significantly higher apoptosis rate (Fig. 2L) compared to the oe-NC group. The above results suggest that overexpression of RARB inhibits the stem cell properties of CSCs and improves radiotherapy sensitivity.

Overexpression of RARB improves the sensitivity of CSCs to radiotherapy *in vivo*

The modulation of RARB on sensitivity to radiotherapy was examined *in vivo* by developing a nude mouse xenograft tumor model, followed by radiation therapy. Relative to the LV-oe-NC group, the mice in the LV-oe-RARB group showed much slower tumor growth and a significant decline in tumor volume (Fig. 3A–C). Moreover, the expression of RARB was much higher in the tumor tissues of mice injected with LV-oe-RARB (Fig. 3D–E). In contrast, the expression of CD133, CD44, and Nanog was significantly decreased (Fig. 3F). The TUNEL assay showed that the apoptosis rate was significantly elevated in the LV-sh-RARB group compared with the LV-sh-NC group (Fig. 3G). It indicates that overexpression of RARB can improve the sensitivity of CSCs to radiotherapy *in vivo*.

RARB promoter is highly methylated in CSCs isolated from CRC cells

In UALCAN (http://ualcan.path.uab.edu/index.html), we queried that the promoter methylation of RARB was significantly elevated in CRC (Fig. 4A). The CpG island on the RARB promoter was subsequently predicted using MethPrimer 2.0 (http://www.urogene.org/methprimer2/index.html) (Fig. 4B). The methylation levels

HCT116 cells and CSCs after radiotherapy (6 Gy) treatment. (D-E) Expression of RARB in HCT116 cells and CSCs treated with radiotherapy (6 Gy) was detected by RT-qPCR and Western blot. CSCs were transfected with oe-NC or oe-RARB and treated with radiotherapy (6 Gy). (F-G) RARB expression in CSCs after transfection was detected by RT-qPCR (F) and Western blot (G). (H) The spheroid formation ability of CSCs after transfection. (I) The expression of stem cell-related factors CD133, CD44 and Nanog in CSCs after transfection was detected by Western blot. (J) The fraction of $CD133^+/CD44^+$ cells in CSCs after transfection was detected by flow cytometry. (K) The clonogenic ability and survival fraction of CSCs after transfection. (L) The apoptosis rate of CSCs after transfection was detected by flow cytometry. The statistical data were expressed as mean ± SD. The differences between two groups were compared by unpaired *t* test, and the others were compared by two-way ANOVA. *, $P < 0.05$.

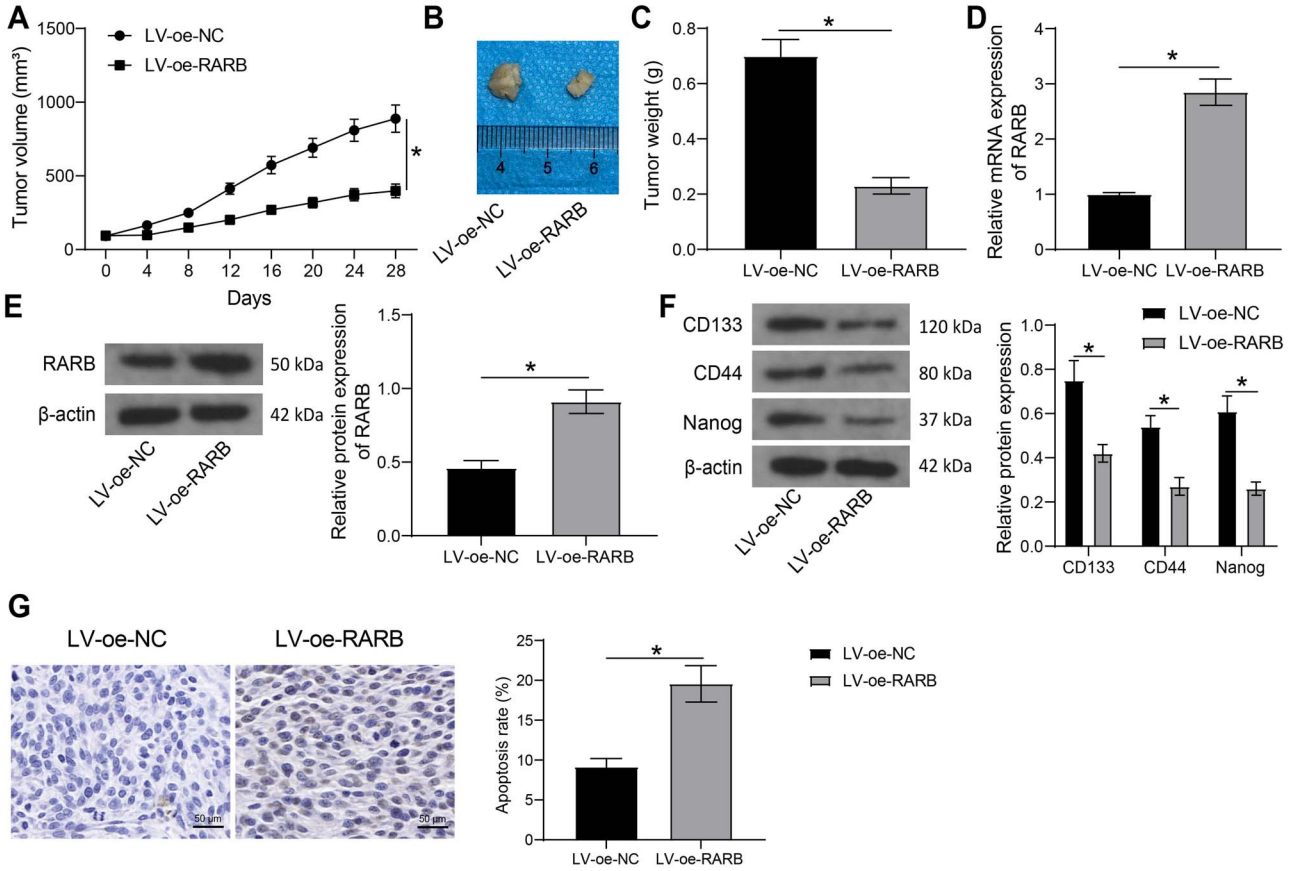

Fig. 3. Overexpression of RARB improves *in vivo* radiotherapy sensitivity of CSCs. (A) The tumor growth curves. (B) Representative images of tumors. (C) Results of tumor weights. (D-E) Detection of RARB expression in tumor tissues by RT-qPCR (D) and Western blot (E). (F) The expression of CD133, CD44 and Nanog in tumor tissues measured using Western blot. (G) The cell apoptosis in tumor tissues examined using TUNEL. The statistical data were expressed as mean ± SD ($n = 6$). The differences between two groups were compared by unpaired *t* test, and the others were compared by two-way ANOVA. *, $P < 0.05$.

of RARB in HIEC-6 cells, HCT116 cells and CSCs were examined using BSP and MSP assays. Consistent with the prediction results, the methylation levels of RARB were significantly higher in HCT116 cells than that in HIEC-6 cells, and were similarly higher in CSCs than that in HCT116 cells (Fig. 4C–D).

To establish whether the decline of RARB expression was caused by its promoter hypermethylation, CSCs were treated with 5-AzaC or control DMSO. The methylation level of RARB was significantly reduced after 5-AzaC treatment (Fig. 4E–F). Meanwhile, the results of RT-qPCR and Western blot assays showed that the expression of RARB was significantly elevated after 5-AzaC treatment (Fig. 4G–H). These results suggest that the RARB promoter is highly methylated in CSCs in CRC.

DNMT1 represses RARB expression through DNA promoter methylation

To determine the potential role of DNMTs in mediating RARB promoter methylation in CRC, the correlation between RARB expression and DNMT1, DNMT3A, DNMT3B expression in CRC was analyzed by StarBase's Pan-cancer platform (https://starbase.sysu.edu.cn/panCancer.php). We observed that DNMT1 expression was significantly and negatively correlated with RARB expression (Fig. 5A). To further determine which DNMT exerts regulatory effects on RARB expression, CSCs were delivered with siRNAs targeting *DNMT1*, *DNMT3A* or *DNMT3B*, respectively. Western blot was conducted to assess the transfection efficacy. The siRNAs with higher silencing efficiency (si-DNMT1#2, si-DNMT3A#2, si-DNMT3B#2) were selected for subsequent assays (Fig. 5B–D). The expression of RARB was significantly elevated after silencing of DNMT1, while no significant changes were observed after silencing of DNMT3A or DNMT3B (Fig. 5E–F). Therefore, it was hypothesized that DNMT1 repressed RARB expression through promoter DNA methylation. Finally, ChIP assay revealed that DNMT1 was recruited in the RARB promoter region (Fig. 5G).

Inhibition of DNMT1 activity improves radiotherapy sensitivity by promoting RARB expression

To verify the role of DNMT1 in regulating radiotherapy sensitivity, we subsequently conducted rescue experiments. RARB expression

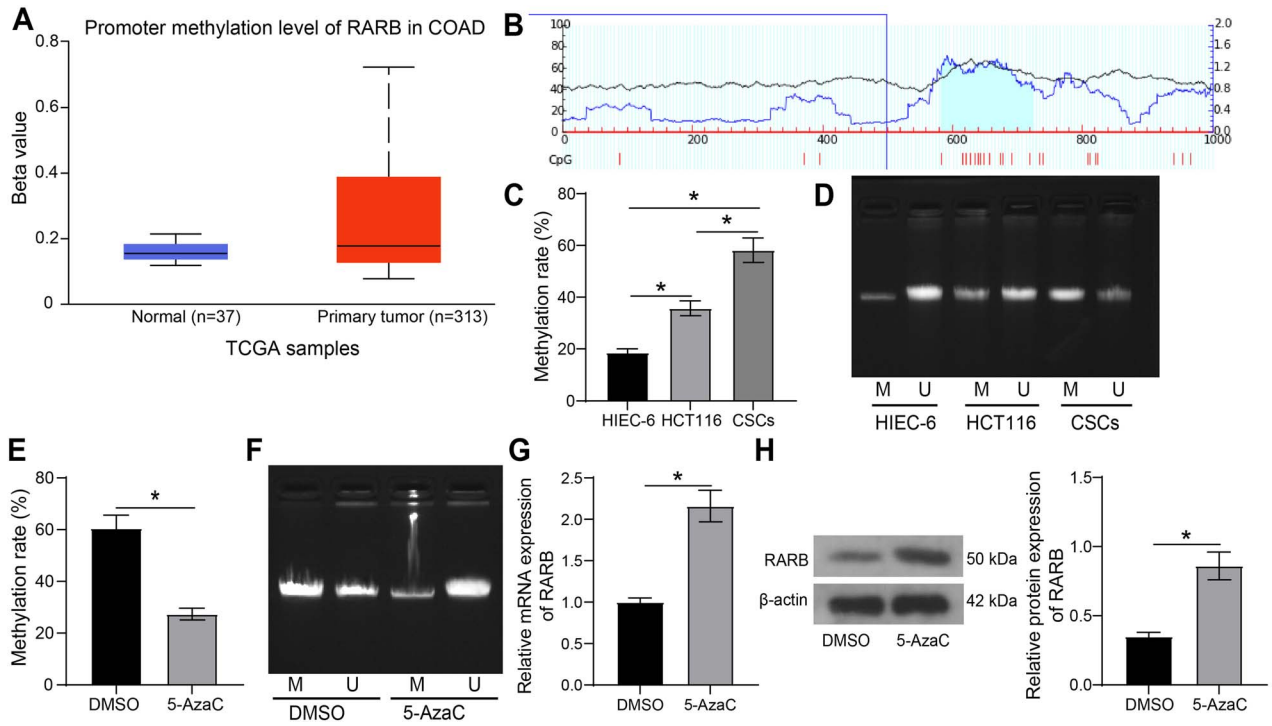

Fig. 4. RARB promoter is highly methylated in CSCs in CRC. (A) The promoter methylation levels of RARB in CRC queried using UALCAN (http://ualcan.path.uab.edu/index.html). (B) Predicted CpG islands on RARB promoters by MethPrimer 2.0 (http://www.urogene.org/methprimer2/index.html). (C–D) The methylation level of RARB in HIEC-6 cells, HCT116 cells and CSCs measured using BSP assay and MSP assay. (E–F) Methylation levels of RARB in CSCs were detected by BSP assay and MSP assay after treatment with 5-AzaC or DMSO. (G–H) RARB expression in CSCs in response to 5-AzaC or DMSO detected using RT-qPCR and Western blot. The statistical data were expressed as mean ± SD. The differences between two groups were compared by unpaired *t* test, and the others were compared by one-way ANOVA. *, $P < 0.05$.

was first detected in CSCs delivered with siRNAs targeting RARB using RT-qPCR. The si-RARB-2 with higher silencing efficiency was selected for subsequent experiments (Fig. 6A) (herein termed si-RARB). Then 5-AzaC-treated CSCs were transfected with si-NC or si-RARB, followed by radiotherapy (6 Gy). The results of RT-qPCR and Western blot assays showed that RARB expression was significantly increased by 5-AzaC treatment, and transfection with si-RARB significantly decreased RARB expression (Fig. 6B–C). Then, the spheroid-forming ability was examined, and it was found that the number of spheroids formed by CSCs were significantly reduced after 5-AzaC treatment (Fig. 6D), while the expression of CD133, CD44 and Nanog in the cells and the fraction of $CD133^{+}CD44^{+}$ cells was also significantly reduced (Fig. 6E–F). Transfection with si-RARB then reversed the repressive effect of 5-AzaC on the stem cell properties of CSCs (Fig. 6D–F). In addition, the results of clonogenic assay and flow cytometry presented that the clonogenic ability and survival fraction of CSCs were significantly reduced after 5-AzaC treatment (Fig. 6G) and the apoptosis rate was significantly augmented (Fig. 6H). In contrast, the clonogenic capacity and survival fraction of CSCs were significantly elevated after transfection with si-RARB (Fig. 6G) and the apoptosis rate was significantly hampered (Fig. 6H). It indicates that 5-AzaC treatment inhibits DNMT1 activity and then improves radiotherapy sensitivity by promoting the expression of RARB.

Inhibition of DNMT1 activity improves *in vivo* radiotherapy sensitivity by suppressing methylation of the RARB promoter

Finally, a subcutaneous xenograft tumor model was constructed to validate the above mechanism *in vivo*. Compared with the DMSO group, tumor growth was significantly slower and tumor volume was significantly reduced in the 5-AzaC group; whereas LV-sh-RARB promoted tumor growth (Fig. 7A–C). Moreover, RARB expression was significantly increased by 5-AzaC treatment, while LV-sh-RARB significantly decreased RARB expression (Fig. 7D–E). Meanwhile, the expression of CD133, CD44 and Nanog was significantly reduced after 5-AzaC treatment, which were upregulated in the presence of LV-sh-RARB (Fig. 7F). Meanwhile, TUNEL results showed that the apoptosis rate increased significantly after 5-AzaC treatment, while LV-sh-RARB inhibited apoptosis (Fig. 7G). The above results suggest that inhibition of DNMT1 activity improves *in vivo* radiotherapy sensitivity by promoting RARB expression.

DISCUSSION

CSCs are major contributors to tumor stemness by enhancing colony formation, proliferation and therapy-resistance [13]. A recent review has highlighted that epigenetics modifications, including DNA

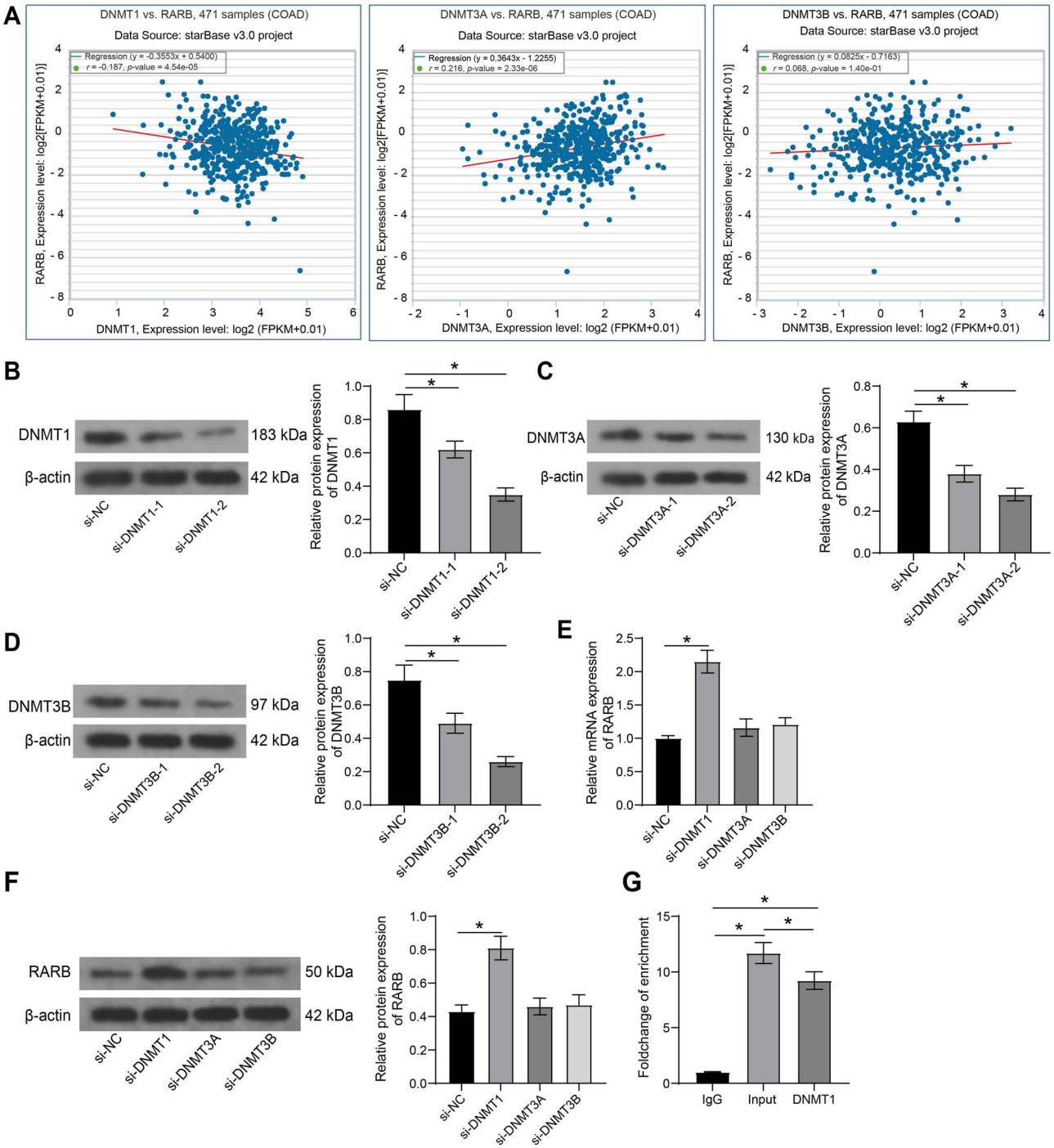

Fig. 5. DNMT1 represses RARB expression through DNA promoter methylation. (A) The correlation between RARB expression and DNMT1, DNMT3A and DNMT3B expression in CRC analyzed using StarBase's Pan-cancer platform (https://starbase.sysu.edu.cn/panCancer.php). (B–D) The expression of DNMT1, DNMT3A and DNMT3B in CSCs transfected with si-DNMT1, si-DNMT3A or si-DNMT3B, respectively measured using western blot. (E–F) The expression of RARB in CSCs transfected with si-*DNMT1*, si-*DNMT3A* or si-*DNMT3B*, respectively measured using RT-qPCR and western blot. (G) DNMT1 recruitment in the RARB promoter region in CSCs determined using ChIP assay. The statistical data were expressed as mean ± SD, the differences between two groups were compared by one-way ANOVA. *, $P < 0.05$.

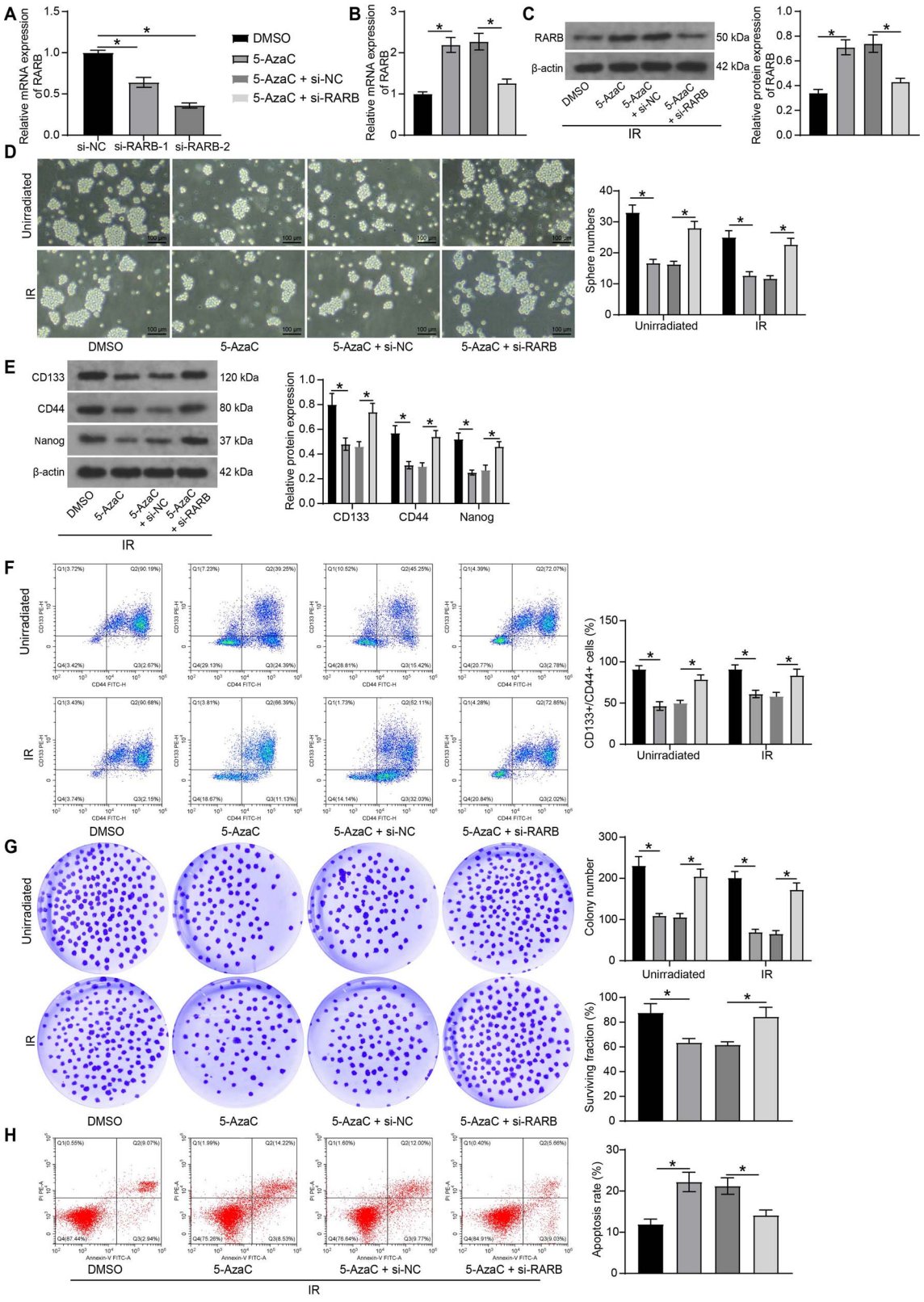

Fig. 6. Inhibition of DNMT1 activity improves radiotherapy sensitivity by promoting RARB expression. (A) The expression of RARB in CSCs delivered with siRNAs targeting RARB. (B-C) RARB expression in CSCs treated with 5-AzaC, si-RARB and 6 Gy

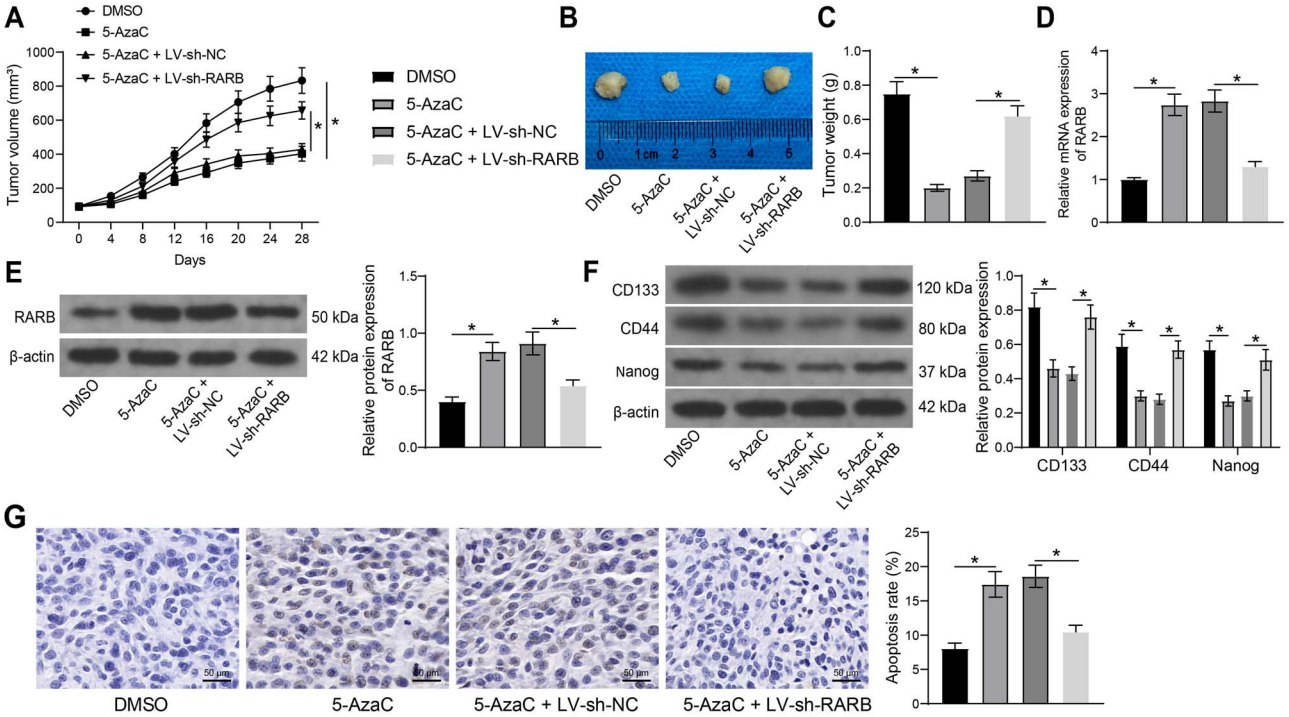

Fig. 7. Inhibition of DNMT1 activity improves *in vivo* radiotherapy sensitivity by suppressing methylation of the RARB promoter. (A) The tumor growth curves. (B) Representative images of tumors. (C) Results of tumor weights. (D–E) Detection of RARB expression in tumor tissues by RT-qPCR and Western blot. (F) The expression of CD133, CD44 and Nanog in tumor tissues measured using Western blot. (G) The cell apoptosis in tumor tissues examined using TUNEL. The statistical data were expressed as mean ± SD ($n = 6$), the differences between multiple groups were compared by one-way or two-way ANOVA. *, $P < 0.05$.

methylation, histone modifications and RNA methylations are main drivers in the maintenance of CSCs [14]. Hence, identifying CSCs and targeting epigenetic pathways might offer new insights into the treatment strategy for CRC. In the present study, we aimed to shed light on the mechanism of how RARB dysregulation affects stemness maintenance of CSCs and radio-resistance. Our findings provided evidence indicating that loss of DNMT1 could reduce methylation of RARB promoter and enhance the expression of RARB, thus repressing stemness maintenance of CSCs and radio-resistance in CRC.

The observation of this study indicated that RARB was downregulated in CRC cells, and the alteration was more pronounced in CSCs. In this work, we found that overexpression of RARB in CSCs suppressed the clonogenic ability, promoted apoptosis and decreased the tumor growth and radio-resistance in nude mice. Nanog plays a dominant role in regulating pluripotency, and CD133 has well-documented associations with cancers, CSCs and chemoresistance. Meanwhile, CD44 is of specific relevance to CRC [15]. Here, we observed that overexpression of RARB lowered the expression of these CSC markers. microRNA-146 induced bladder cancer cell proliferation and invasion by targeting RARB [16]. Mori *et al.* also found a combination of six genes, including RARB could distinguish oral cancer from clinically diagnosed oral potentially malignant disorders with high diagnostic performance [17]. In addition, polymethoxyflavones extracted from citrus inhibited gastric cancer cell proliferation through triggering apoptosis by upregulating RARB *in vitro* and *in vivo* [18]. Doan *et al.* suggested that overexpression of RARB was related to improved breast cancer-specific survival, which may represent as an attractive target for the treatment of breast cancers that are refractory to current therapeutic options [19]. However, the regulatory effects of RARB on the stemness of CSCs remains largely unclear, which highlighted the novelty of our study. Rybicki *et al.* demonstrated that the methylation of the RARB gene significantly increased risk of biochemical recurrence

IR was detected by RT-qPCR and Western blot. (D) The spheroid formation ability of CSCs after transfection and 5-AzaC treatment. (E) The expression of stem cell-related factors CD133, CD44 and Nanog in CSCs after transfection and 5-AzaC treatment was detected by Western blot. (F) The fraction of $CD133^+/CD44^+$ cells in CSCs after transfection and 5-AzaC treatment was detected by flow cytometry. (G) The clonogenic ability and survival fraction of CSCs after transfection and 5-AzaC treatment. (H) The apoptosis rate of CSCs after transfection and 5-AzaC treatment was detected by flow cytometry. The statistical data were expressed as mean ± SD, the differences between multiple groups were compared by one-way or two-way ANOVA. *, $P < 0.05$.

in African American men diagnosed with prostate cancer [20]. In combination with our prediction and experimental results, we believed that the decline of RARB in CRC cells and the extracted CSCs were caused by hypermethylation of its promoter CpG island. Our following assays using 5-AzaC further supported our hypothesis. Interestingly, Park *et al.* revealed that RARB was one of the 15 promoter CpG island loci showed high methylation status in breast cancer progression, and methylation of promoter CpG islands was significantly lower in $CD44^+/CD24^+$ cell tumors than in $CD44^+/CD24^-$ cell tumors, even within the basal-like subtype [21]. Even though we did not reveal the detailed mechanism of RARB regulating CD133/CD44 levels and radio-resistance, we managed to provide the direct evidence between RARB overexpression and the suppressed CSCs activity and radio-resistance.

Using correlation analysis, RT-qPCR and western blot, we identified DNMT1 as the upstream factor determining the methylation status and the expression of RARB in CRC and CSCs. DNMT1 was recruited in the HOXD10 promoter, and demethylation by 5-Aza-2′-deoxycytidine can sufficiently induce HOXD10 expression in CRC cells [22], which was quite in line with our observation. DNMT1-catalyzed methylation has been implicated in the stemness and radio-resistance in diverse cancers, including liver cancer [23], breast cancer [24], as well as head and neck cancer [25]. More importantly, DNMT1 maintained the methylation of microRNA-152-3p, thereby affecting the biological characteristics of CRC cells [26]. Combined inhibition of DNMT1 and HDAC1 using genetic depletion or inhibitors boosted the inhibiting effects on proliferative capacity of head and neck cancer cells and *in vivo* tumorigenesis after irradiation [27]. Similarly, the silencing of long non-coding RNA DLX6-AS1 inhibited spheroid formation, colony formation, proliferation and tumor formation, and attenuated the expression of CD133 and Nanog in liver CSCs, which was elicited through a decline in CADM1 promoter methylation by inhibiting DNMT1 expression [28]. In the current study, we applied 5-AzaC, a compound that has the potential to cause hypomethylation [29], to treat CSCs alone or in combination with si-RARB. As expected, inhibition of methylation using 5-AzaC led to partial loss of stemness and resistance to irradiation, which was reversed by RARB knockdown. The combined administration of 5-AzaC and IR significantly hampered tumor growth in the mouse xenograft model, and promoted radiation-induced apoptosis of nasopharyngeal carcinoma cells *in vitro* compared to 5-AzaC alone or IR alone [30]. These findings supported the conception that 5-AzaC plays a radiation-sensitizing role in CRC via the hypomethylation of RARB.

CONCLUSION

We discovered a novel epigenetic pathway that DNMT1 could hypermethylate the promoter region of RARB in CSCs, thereby coordinating CSC stemness and participating in radiation resistance. Therefore, these data suggest that RARB may be a potential therapeutic target for CRC. Still, the mechanism of RARB on CSC stemness and radiation resistance should be investigated carefully.

FUNDING

This work was supported by National Natural Science Foundation of China (No. 81760442).

CONFLICT OF INTEREST

The authors declare they have no conflicts of interest.

ACKNOWLEDGMENTS

Authors are thankful to the National Natural Science Foundation of China (No. 81760442).

REFERENCES

1. Siegel RL, Miller KD, Goding Sauer A et al. Colorectal cancer statistics, 2020. *CA Cancer J Clin* 2020;70:145–64.
2. Siegel RL, Miller KD, Fuchs HE et al. Cancer statistics, 2021. *CA Cancer J Clin* 2021;71:7–33.
3. Chen Y, Zheng X, Wu C. The Role of the tumor microenvironment and treatment strategies in colorectal cancer. *Front Immunol* 2021;12:792691.
4. Fanale D, Castiglia M, Bazan V et al. Involvement of non-coding RNAs in chemo- and radioresistance of colorectal cancer. *Adv Exp Med Biol* 2016;937:207–28.
5. Walcher L, Kistenmacher AK, Suo H et al. Cancer stem cells-origins and biomarkers: perspectives for targeted personalized therapies. *Front Immunol* 2020;11:1280.
6. Desai A, Yan Y, Gerson SL. Concise reviews: cancer stem cell targeted therapies: toward clinical success. *Stem Cells Transl Med* 2019;8:75–81.
7. Fu L, Shi Z, Chen B. Deleted in lymphocytic leukemia 2 induces retinoic acid receptor beta promoter methylation and mitogen activated kinase-like protein activation to enhance viability and mobility of colorectal cancer cells. *Bioengineered* 2022;13:12847–62.
8. Easwaran H, Tsai HC, Baylin SB. Cancer epigenetics: tumor heterogeneity, plasticity of stem-like states, and drug resistance. *Mol Cell* 2014;54:716–27.
9. Cabrera-Licona A, Perez-Anorve IX, Flores-Fortis M et al. Deciphering the epigenetic network in cancer radioresistance. *Radiother Oncol* 2021;159:48–59.
10. Rasmussen SL, Krarup HB, Sunesen KG et al. Hypermethylated DNA, a circulating biomarker for colorectal cancer detection. *PLoS One* 2017;12:e0180809.
11. Subramaniam D, Thombre R, Dhar A et al. DNA methyltransferases: a novel target for prevention and therapy. *Front Oncol* 2014;4:80.
12. Wang Y, Wang J, Yang L et al. Epigenetic regulation of intestinal peptide transporter PEPT1 as a potential strategy for colorectal cancer sensitization. *Cell Death Dis* 2021;12:532.
13. Deldar Abad Paskeh M, Asadi S, Zabolian A et al. Targeting cancer stem cells by dietary agents: an important therapeutic strategy against human malignancies. *Int J Mol Sci* 2021;22:11669.
14. Keyvani-Ghamsari S, Khorsandi K, Rasul A et al. Current understanding of epigenetics mechanism as a novel target in reducing cancer stem cells resistance. *Clin Epigenetics* 2021;13:120.
15. Munro MJ, Wickremesekera SK, Peng L et al. Cancer stem cells in colorectal cancer: a review. *J Clin Pathol* 2018;71:110–6.
16. Shan L, Liu W, Zhan Y. LncRNA HAND2-AS1 exerts anti-oncogenic effects on bladder cancer via restoration of RARB as a sponge of microRNA-146. *Cancer Cell Int* 2021;21:361.

17. Mori K, Hamada T, Beppu M et al. Detecting early-stage oral cancer from clinically diagnosed oral potentially malignant disorders by DNA methylation profile. *Cancers (Basel)* 2022;14:2646.
18. Wang Y, Chen Y, Zhang H et al. Polymethoxyflavones from citrus inhibited gastric cancer cell proliferation through inducing apoptosis by upregulating RARbeta, both in vitro and in vivo. *Food Chem Toxicol* 2020;146:111811.
19. Doan TB, Cheung V, Clyne CD et al. A tumour suppressive relationship between mineralocorticoid and retinoic acid receptors activates a transcriptional program consistent with a reverse Warburg effect in breast cancer. *Breast Cancer Res* 2020;22:122.
20. Rybicki BA, Rundle A, Kryvenko ON et al. Methylation in benign prostate and risk of disease progression in men subsequently diagnosed with prostate cancer. *Int J Cancer* 2016;138:2884–93.
21. Park SY, Kwon HJ, Choi Y et al. Distinct patterns of promoter CpG island methylation of breast cancer subtypes are associated with stem cell phenotypes. *Mod Pathol* 2012;25:185–96.
22. Pan W, Wang K, Li J et al. Restoring HOXD10 exhibits therapeutic potential for ameliorating malignant progression and 5-fluorouracil resistance in colorectal cancer. *Front Oncol* 2021;11:771528.
23. Wang Q, Liang N, Yang T et al. DNMT1-mediated methylation of BEX1 regulates stemness and tumorigenicity in liver cancer. *J Hepatol* 2021;75:1142–53.
24. Liu H, Song Y, Qiu H et al. Downregulation of FOXO3a by DNMT1 promotes breast cancer stem cell properties and tumorigenesis. *Cell Death Differ* 2020;27:966–83.
25. Kim SH, Kang BC, Seong D et al. EPHA3 contributes to epigenetic suppression of PTEN in radioresistant head and neck cancer. *Biomolecules* 2021;11:599.
26. Wang C, Ma X, Zhang J et al. DNMT1 maintains the methylation of miR-152-3p to regulate TMSB10 expression, thereby affecting the biological characteristics of colorectal cancer cells. *IUBMB Life* 2020;72:2432–43.
27. Lee M, Nam HY, Kang HB et al. Epigenetic regulation of p62/SQSTM1 overcomes the radioresistance of head and neck cancer cells via autophagy-dependent senescence induction. *Cell Death Dis* 2021;12:250.
28. Wu DM, Zheng ZH, Zhang YB et al. Down-regulated lncRNA DLX6-AS1 inhibits tumorigenesis through STAT3 signaling pathway by suppressing CADM1 promoter methylation in liver cancer stem cells. *J Exp Clin Cancer Res* 2019;38:237.
29. Klutstein M, Nejman D, Greenfield R et al. DNA Methylation in cancer and aging. *Cancer Res* 2016;76:3446–50.
30. Jiang W, Li YQ, Liu N et al. 5-Azacytidine enhances the radiosensitivity of CNE2 and SUNE1 cells in vitro and in vivo possibly by altering DNA methylation. *PLoS One* 2014;9:e93273.